

Supporting Information

Plasmon-Resonance-Enhanced Circularly Polarized Luminescence of Self-Assembled Meso-tetrakis(4-sulfonatophenyl)porphyrin-Surfactant Complexes in interaction with Ag Nanoparticles

Takunori Harada,*^a Naoki Kajiyama,^a Kei Ishizaka,^b Reona Toyofuku,^b Katsuki Izumi,^b Kazuo Umemura,^b Yoshitane Imai,^c Naoya Taniguchi^c and Kenji Mishima^a

^aDepartment of Chemical Engineering, Fukuoka University, 8-19-1 Nanakuma, Jonan-ku, Fukuoka 814-0180, Japan. Fax: (+81) 3 5465 7654; E-mail: tharada@fukuoka-u.ac.jp

^bTokyo University of Science, 1-3 Kagurazaka, Shinjuku, Tokyo, 162-8601 Japan.

^cDepartment of Applied Chemistry, Faculty of Science and Engineering, Kinki University, 3-4-1 Kowakae, Higashi-Osaka, Osaka 577-8502, Japan.

Table of Contents

1. Experimental Section	S2-S4
1.1 Materials, instrumentation and techniques	S2
1.2 Synthetic procedure and characterization data	S2-S4
2. Figures	S5-S8
3. References	S9

1. Experimental Section

1.1 Materials, instrumentation and techniques

The 5,10,15,20-tetrakis(4-sulfonatophenyl)porphyrin (TPPS) was purchased from STEM chemical Co. Ltd. The cationic surfactants of cetyltrimethylammonium bromide (CTAB) and (-)-(1*R*,2*S*)-*N*-Dodecyl-*N*-methylephedrinium bromide ((-)-DMEB) were purchased from Sigma-Aldrich. They were used without further purification.

All the polarization phenomena of CD and circularly polarized luminescence (CPL) were measured on the homemade chiroptical spectrophotometer (CPL-200CD)¹, CD spectrophotometer (J-1500) and CPL spectrophotometer (CPL-200). The methods for obtaining true CD and CPL spectra, based on the Stokes-Mueller matrix analysis, have been reported in our previous paper.² The CD spectra were recorded over a wavelength range of 600-350 nm with 'Standard' sensitivity at 50 nm/min scan speed with 1 nm resolution and time constant of 1 s. The CPL spectra were recorded over a wavelength range of 800-550 nm with 'Standard' sensitivity at 20 nm/min scan speed with 10 nm resolution and time constant of 4 s. Data were further processed for noise reduction if necessary. The CD and CPL signals were presented in ellipticities (mdeg). Parasitic signals which were originated from the coupling effect between non-ideal characteristics of optical components and intrinsic macroscopic anisotropies (LB, LD and LPL), and thus contained in the recorded CD and CPL signals were removed.

FT-IR and UV-vis absorption measurements were performed by FT-IR (FT-IR 470Plus) and UV-Vis (V-550: Jasco) spectrophotometers. A Honeywell Microtrac UPA 150 dynamic light scattering (DLS) particle size analyzer was used to measure the particle size distribution. Particles were diluted in deionized water and then sonicated for 5 min before sizing.

AFM observations were carried out with a commercially available AFM (MFP-3D microscope, Asylum Research, CA, USA), equipped with a vertical-engage J scanner. A silicon (20 to 40 N/m) cantilever (PPP-NCSTR-W (NANOSENSORS, NanoWorld AG, Neuchâtel, Switzerland)) was used for tapping mode in air. Force values for imaging and scratching were estimated by force curve measurements. Imaging in air was carried out in tapping mode or contact mode. The AFM unit was stored in a plastic chamber when the humidity was controlled during measurements.

1.2 Synthetic procedure and characterization data

Synthesis

(+)-DMEB was prepared in 53 % overall yields from (1*S*,2*R*)-(+)-norephedrine by using the previously reported method (see Fig. S1).^{3,4}

Synthesis I (NPs)

Citrate-capped silver NPs synthesis was performed by a following procedure: a 19.8 mL of 1.0 mM AgNO₃ aqueous solution was mixed with a 0.2 mL of 1 M trisodium citrate dehydrate solution, and then 50 μ L of ice-cooled 0.24 M NaBH₄ aqueous solution was added, yielding pale brown seed solution. This solution was maintained at 0 °C throughout the preparation. Ultra-pure deionized water was used to prepare all aqueous solutions.

In order to get more direct evidence for the particle size, the dispersed AgNPs was examined using DLS particle size analyzer and UV-Vis spectroscopy. Fig. S7 indicates UV-Vis absorption spectrum and particle distribution of the dispersed AgNPs in aqueous solution. The UV-Vis absorption spectrum shows evidence that the individual NPs are spherical particles with approximate sizes of ~ 10 nm, giving very good agreement with DSL data.

Synthesis II (TPPS *J*-aggregate interacted with DMEB)

At a concentration greater than 1×10^{-5} M, dianion H_4TPPS^{2-} molecules in an acidic aqueous solution form chiral *J*-aggregates $(TPPS)_n$, which exhibit a quite narrow Soret band ($B_J \approx 489$ nm) attributed to intermolecular interaction between transition dipole moments causing a delocalization of excitons over the aggregates.⁵ The handedness of their chirality can be finely controlled by the electrostatic interaction with cationic chiral surfactants, (-)- or (+)-DMEB as shown previously reported.⁶ The $(TPPS)_n$ -DMEB complex was produced in the presence of the already formed $(TPPS)_n$ aqueous solution (1.0 mL of 0.03 mM, pH 2.3) by addition of 1.0 mL of 0.03 mM DMEB aqueous solution. (0.034 mM $<$ cmc (0.4 mM)). The electrostatic attraction between these two oppositely-charged materials provides the driving force to form a stable $(TPPS)_n$ -surfactant complex. The stoichiometric ratio of TPPS to DMEB was adjusted to 1:1. However, when the concentration ratio of TPPS and DMBE was above 1:2, the $(TPPS)_n$ -surfactant complex was less stable than 1:1 over a long period of time.

Synthesis III (composite $(TPPS)_n$ -DMEB/NPs)

Finally, the TPPS *J*-aggregate $(TPPS)_n$ -DMEB was electrostatically bound to the citrate-capped AgNPs by adding 2 mL of a 0.015 mM $(TPPS)_n$ -DMEB to the Ag nanoparticle aqueous solution. In this case, the DMEB displaced most of the citrate bound to the surface of the AgNPs. A reference solution of 0.03 mM $(TPPS)_n$ -DMEB was prepared by diluting stock solution with acidic aqueous solution (pH = 2.3). The stoichiometric ratio of TPPS to NPs was adjusted to 1:5.

Characterization

CD and CPL measurements were performed on a home-made chiroptical spectrophotometer (CPL-200CD) based on J-720 (JASCO) in a 10 mm fused silica cell. Surfactant binding was also confirmed by Fourier transform infrared (FT-IR) and UV-Vis spectroscopies as shown in Supporting Information Fig. S3 and Fig. S4. FT-IR showed the presence of IR stretching frequencies for the νCH_2 ($3000-2800$ cm^{-1} region) and νRSO_3H ($1080-1000$ cm^{-1} region) bands shifted from that observed in the unbound surfactant and H_4TPPS^{2-} , respectively.⁷ Similarly, a red shifted Soret band ($B_J \approx 491$ nm compared to 489 nm for the free $(TPPS)_n$) and *Q*-band ($Q_J = 715$ nm compared to 711 nm) were observed. Fluorescence measurements were done on a FP-8200 (JASCO).

Samples were prepared for AFM by evaporating 3 μ L of nanoparticle solution (at 25 $^{\circ}C$) on freshly cleaved mica. Atomic force microscopy (AFM) observations were carried out with a commercially available AFM (MFP-3D microscope, Asylum Research, CA, USA), equipped with a vertical-engage J scanner. A silicon (20 to 40 N/m) cantilever was used for tapping mode in air.

To obtain more direct evidence for (TPPS)_n-DMEB/AgNPs composite, (TPPS)_n-DMEB and (TPPS)_n-DMEB/AgNPs on freshly cleaved mica were examined using AFM. Regular rod-shaped structures were observed in AFM image topology of (TPPS)_n-DMEB shown in Fig. S8 (top). The rod-like structures are rectangular in cross section with a thickness of 6 ± 1 nm, breadth of 44 ± 3 nm, and length of \sim hundreds of nm, which is nearly identical to the well-defined rod-like structure (3 nm high, 40-50 nm wide and 0.5-1.5 μ m long) consisting of pure (TPPS)_n.⁸ From the CPK models, the lengths of DMEB molecules in the fully stretched conformation are estimated as 1.8 nm. A plausible explanation may be that the alkyl chains of DMEB adsorbed (TPPS)_n were tilted by ca. 65° to the normal for long axis of *J*-aggregate. The (TPPS)_n-DMEB interacted with AgNPs were also investigated. (TPPS)_n-DMEB/AgNPs composite showed a topography of stick-like form consisting of bundles of rod-like *J*-aggregates having various heights (12 ± 2 nm) and widths (90 ± 5 nm), and of the 2D island-shape (AgNPs clusters) on the rod-like (TPPS)_n-DMEB implying the successful incorporation with AgNPs. (Fig. S8 (bottom)) The AFM images show no evidence for the presence of macroscopic canonical chiral features (helical twisting) which may contribute to the observed induced CD and CPL.

2. Figures and Tables

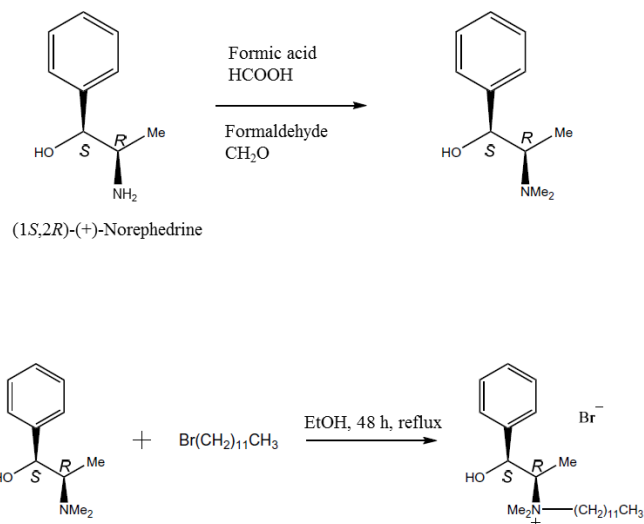


Figure S1. The synthesis route of (1*S*,2*R*)-(+)-*N*-Dodecyl-*N*-methyl-ephedrinium bromide ((+)-DMEB).

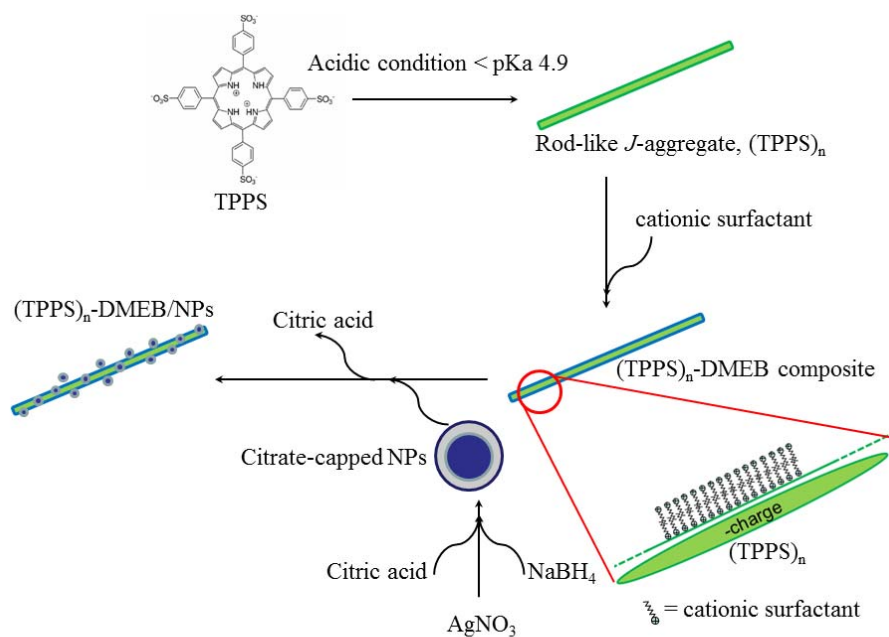


Figure S2. Reaction route to prepare (TPPS)_{*n*}-DMEB/Ag nanocomposite.

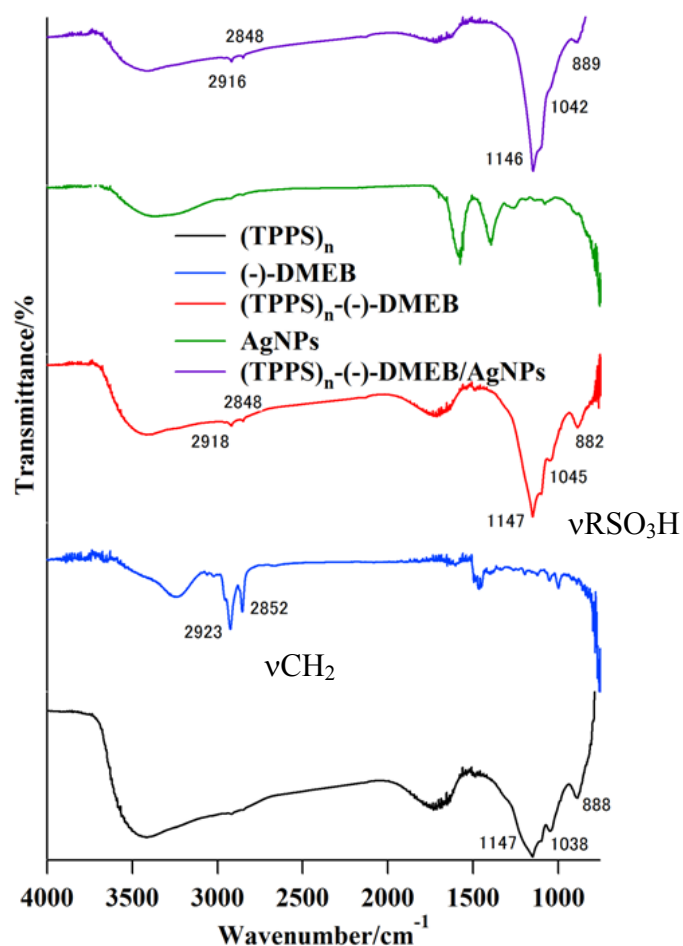


Figure S3. FT-IR spectra of free (TPPS)_n, (-)-DMEB, (TPPS)_n-(-)-DMEB, AgNPs and (TPPS)_n-(-)-DMEB/AgNPs composite. Spectra were collected on a Jasco FT-IR spectrophotometer and averaged over a 50 scans. Samples were prepared by depositing ~2 μL of each solution onto a polished CaF₂ substrate and N₂ gas dried.

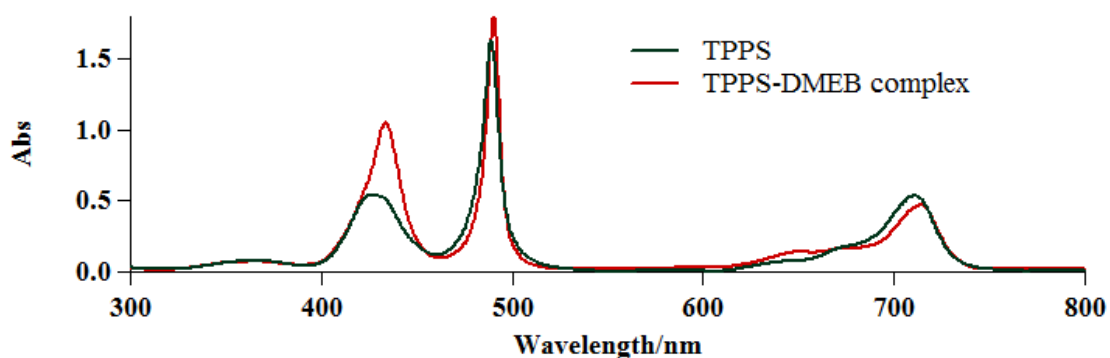


Figure S4. Electronic absorption spectra of free (TPPS)_n and (TPPS)_n-DMEB complex in aqueous solution (pH = 2.3). Spectra were collected on a Jasco UV-Vis spectrophotometer and averaged over a 4 scan.

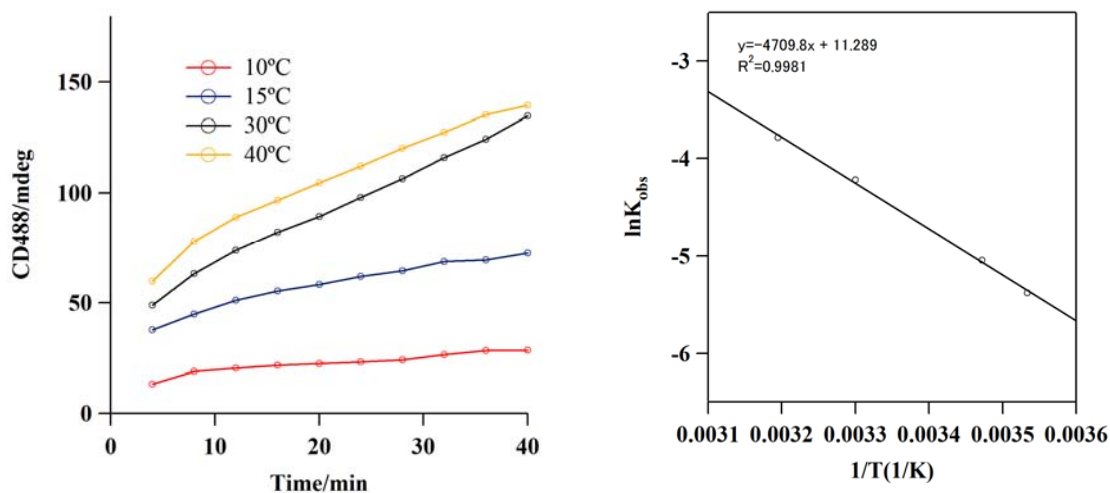


Figure S5. Left) Time dependence of the CD intensity at 488 nm of (TPPS)_n with (-)-DMEB in aqueous solution at 10, 15, 30 and 40 °C; [TPPS] = 0.01 mM, [(-)-DMEB] = 0.01 mM. These measurements were performed by the following procedure; a small amount (1 mL) of the aqueous solution containing TPPS (0.01 mM) and (-)-DMEB (0.01 mM), which was left to stand for over 30 min at room temperature, was added to H₂SO₄ (3 μL) at the desired temperature. Right) Arrhenius plot for the interaction of TPPS and (-)-DMEB.

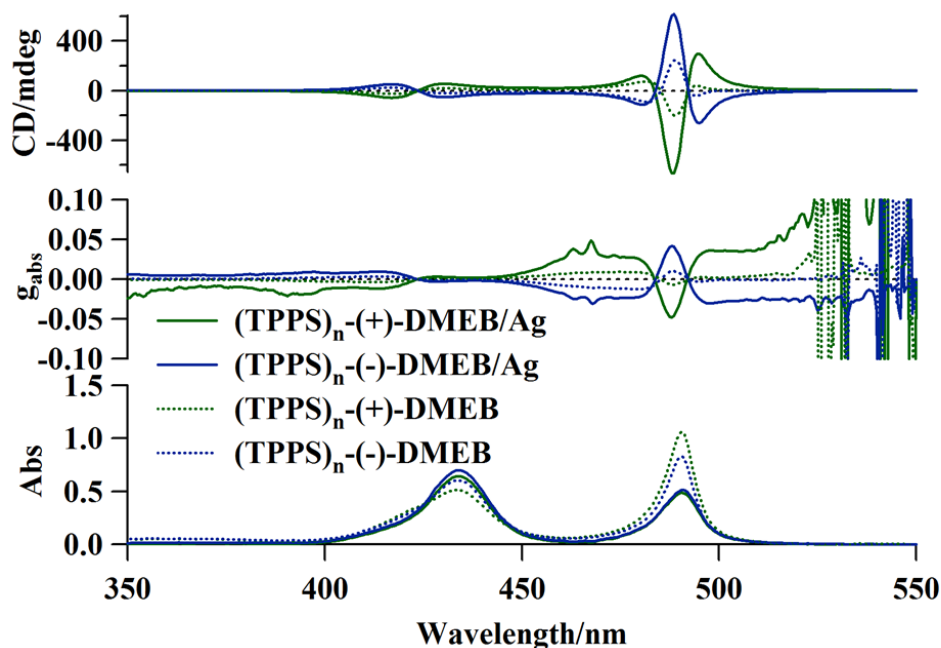


Figure S6. CD spectra of free (TPPS)_n-DMEB and (TPPS)_n-DMEB/AgNPs composite in aqueous solution (pH = 2.3). Spectra were collected on a Jasco J-1500 spectrophotometer.

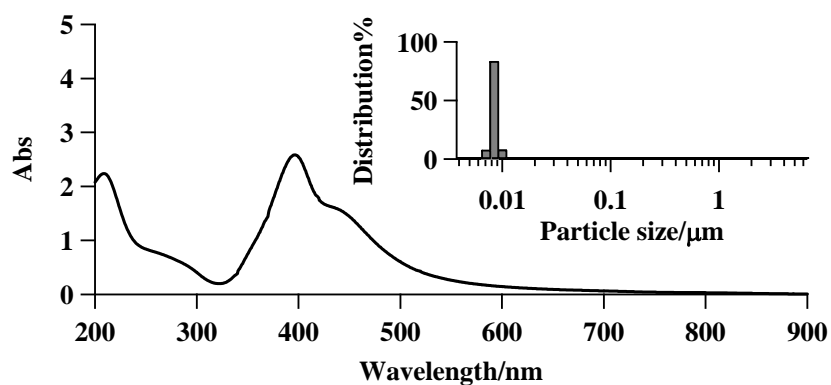


Figure S7. Surface-plasmon-resonance absorption spectrum of silver nanoparticles (AgNPs) dispersed in aqueous solution. [AgNPs] = 0.12 mM. Inset) DLS data plotted graphically indicating particle size range.

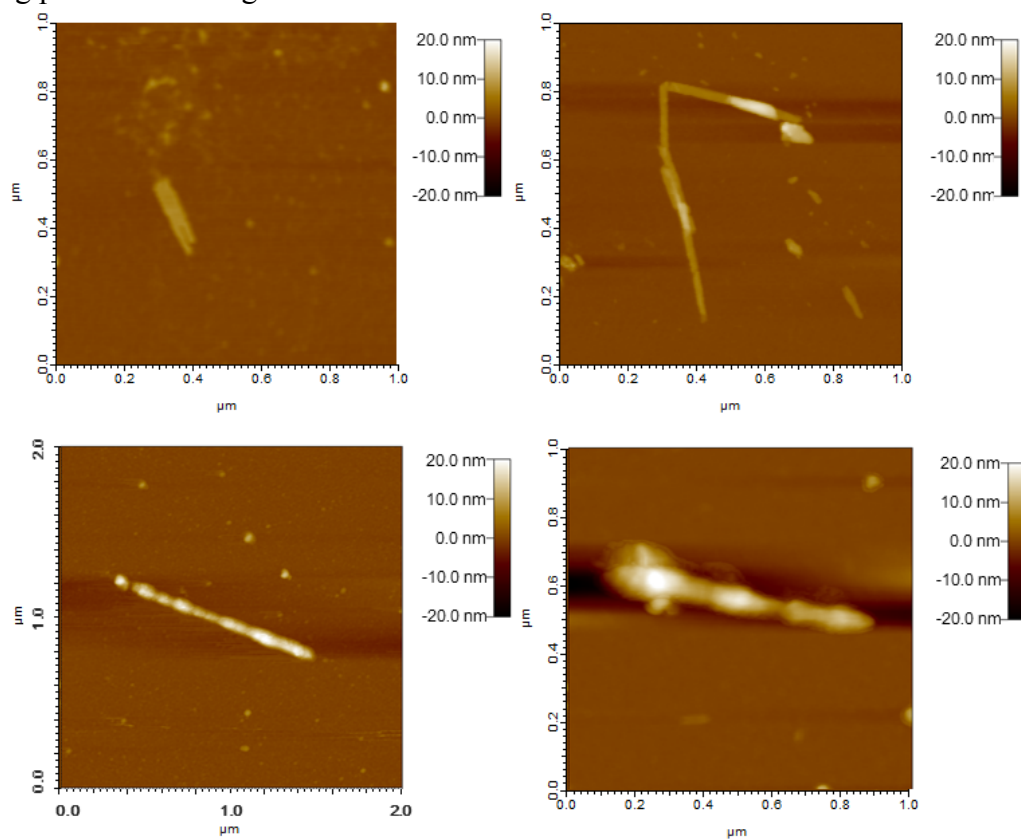


Figure S8. Tapping mode AFM images of (TPPS)_n-DMEB and (TPPS)_n-DMEB/AgNPs on freshly cleaved mica: [TPPS] = 0.01 mM, [DMEB] = 0.01 mM, [AgNPs] = 0.05 mM. Two-dimensional AFM images of the DMEB capped TPPS aggregates without (top) and with (bottom) AgNPs. The image scales are $1 \times 1 \mu\text{m}^2$ or $2 \times 2 \mu\text{m}^2$.

4. References

- ¹ T. Harada, M. Takamoto, H. Hayakawa, M. Watanabe, *Rev. Sci. Instrum.*, to be submitted.
- ² R. Kuroda, T. Harada and Y. Shindo, *Rev. Sci. Instrum.*, 2001, **72**, 3802.
- ³ E. G. Bil, E. C.-Polisini, A. D.-Nowicki, R. Sassine, F. Launay and A. Roucoux, *ChemSusChem.*, 2012, **5**, 91.
- ⁴ A. M. Flock, A. Krebs and C. Bolm, *Synlett.*, 2010, **8**, 1219.
- ⁵ O. Ohno, Y. kaizu, H. Kobayashi, *J. Chem. Phys.* 1993, **99**, 4128.
- ⁶ T. Harada, H. Moriyama, H. Takahashi, K. Umemura, H. Yokota, R. Kawakamia and K. Mishima, *Appl. Spectrosc.*, in press.
- ⁷ N. C. Maiti, S. Mazumdar and N. Periasamy, *J. Phys. Chem. B.*, 1998, **102**, 1528.
- ⁸ J. Crusats, J. Claret, I. Díez-Pérez, Z. El-Hachemi, H. García-Ortega, R. Rubires, F. Sagués, J. M. Ribó, *Chem. Commun.* 2003, 1588.